Matching Problems Between Linac and Compressor Ring

K. Bongardt
Institut für Kernphysik
KFA Jülich, D-52425 Jülich

Abstract

All accelerator schemes, discussed for a next generation spallation neutron source, start with a high current linear accelerator, injecting into a compressor ring or a rapid cycling synchrotron. For loss-free ring injection and extraction, the injector linac has to provide 200 nsec long voids every ring revolution time, typically 1 µsec. In order to keep the trapping voltage down, the outcoming linac bunches have to be rotated, and the energy has to be slowly ramped over the injection cycle. Solutions are presented for a low energy fast chopper, and for a high energy bunch rotator which also ramps the energy. Emphasis is given to the complications due to the high peak and average intensity required. For the beam chopper, different locations are discussed and one design shows how to incorporate the chopper after the RFQ, keeping the beam bunched.

In the transfer line from the linac to the compressor ring, longitudinal space charge forces influence the position and voltage for the bunch rotation cavity. Simple analytical formulae are given to calculate both effects. Longitudinal aberration effects, caused by the sinusoidal voltage, are substantial for energy ramping with the bunch rotation cavity. The correct rotation voltage may be controlled on-line by broadband pickups. In front of the cavity, an achromatic bending system should be installed which allows the scraping of longitudinal halo particles.

1. The Fast Beam Chopper at Low Energies

Next generation spallation neutron sources [1] such as the proposed European Spallation Source ESS [2], start with an RFQ, followed by a drift tube linac (DTL) at ~ 2.5 MeV. Both structures operate at a frequency of ~ 400 MHz and the H^--ion source has to deliver a pulse current of 50 mA at 100 keV. In order to minimize the injection loss in the following ring, a fast chopping device is needed with rise-fall times of about 10 nsec, creating a 200 nsec void every 1 µsec. For locating this device, 3 different positions may be considered:

a) Chopper between ion source and RFQ

Charge neutralization of the ion beam affects beam quality [3-5] so this chopping arrangement is not recommended (even though its chopper voltage requirements are least). However, a "prechopper" at this location reduces the heat load at a down-stream collector after the main chopper; such a "prechopper" should gradually decrease the beam intensity in the 200 nsec void without destroying the neutralization.

b) Chopping at a medium energy

By splitting the 400 MHz RFQ at 1 MeV, the chopper may be installed without affecting the beam quality. The main advantage here is the small chopper length, because the minimal product of voltage, U, length, L, given for a point like chopper by:

$$(U.L)_{min} \sim \quad \varepsilon_t^n \beta \qquad (1)$$

ε_t^n: normalized transverse rms emittance

$\beta \cdot c$ = particle velocity

is 175 V · m for an rms emittance of 0.2 π mm mrad and T = 1 MeV. For the minimal voltage · length value, the chopper and unchopped beam are just separated in phase space. Assuming a rise and falltime of 10 nsec (0-90%) and a voltage gradient of 100 V/nsec, obtained so far with existing chopping devices [3,6], then a chopper length of L = 2 · L min = 35 cm is needed to install a collector about 90° in betatron phase downstream, where the unchopped and chopped beam are well separated in real space. The collector is essential, because for an average current of 5 mA the average power density is ~ 300 W/cm^2.

For a 400 MHz bunched beam with a peak current of 50 mA at 1 MeV, the chopper and collector system is just not feasible. The arrangement cannot be ruled out completely, however, as chopping the coasting beam may be considered. The coasting beam has to be trapped adiabatically in the downstream 400 MHz RFQ; detailed studies are required to assess this possibility.

c) Chopping between RFQ and DTL at 2.5 MeV

The minimum voltage · length value needed is increased to 275 V · m for the same emittance. In addition, the collector now has to absorb an average power density of 750 W/cm^2 for 5 mA average current. In spite of these demands, both chopper and collector may be installed in a transfer line, even for a bunched beam. In Fig. 1, the complete transfer line is shown for a 50 mA bunched beam at 2.5 MeV, including the matching section into the following 400 MHz DTL. A detailed description of this line is given in ref. [7].

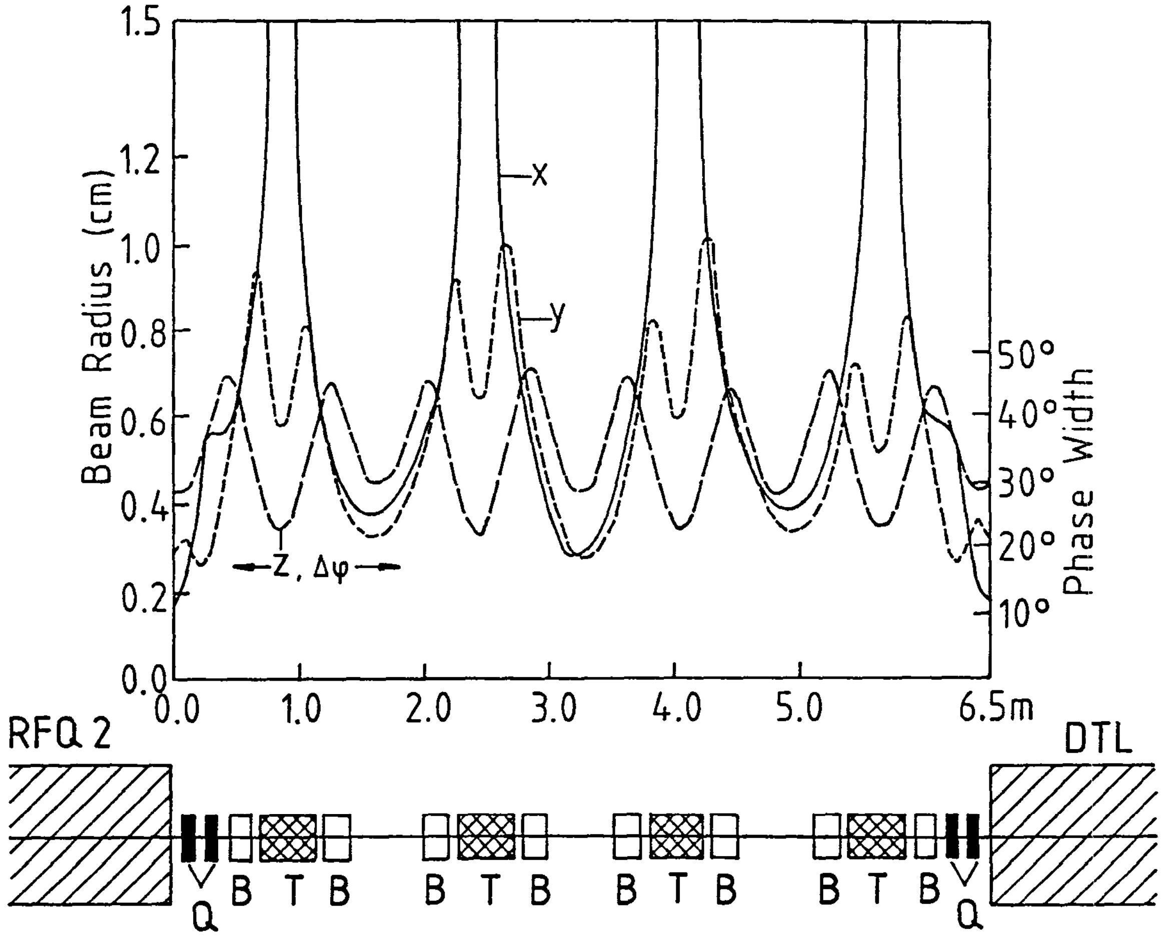

RFQ 2, DTL, B : 400 MHZ, Q quadrupole, T triplet

Fig. 1: Optical elements of the 2.5 MeV transport line, with beam envelopes ($\sqrt{5}$ · rms-value)

The design is basically a "triple waist" in the 0.6 m long drift sections between the buncher (B)-triplet (T)-buncher (B) elements. The fast beam chopper may be installed in the first drift section and the collector in the second. The third drift section is foreseen for moveable diagnostics. Fig. 2 shows the separation between the chopped and unchopped beam at the collector position, assuming a voltage · length value of 750 Vm, which is about 2.5 the minimum value. The transfer line was designed for the European Hadron Facility EHF [8], a Kaon facility with 100 μA average current. As the ESS needs about 5 mA average current, the beam separation at the collector has to be enlarged and care taken with the 4 bunches during the 10 nsec rise time. Both problems may be solved by increasing the chopper length to 0.9 m or 3.5 times the minimum. The voltage is assumed to be 100 V/nsec · 10 nsec = 1 kV. By doing so, the first kicked bunch stays in the linac with small, tolerable oscillations around the axis. Bunches 2 and 3 are destroyed in the transfer line, and bunch 4 is absorbed at the collector. The presented design in Fig. 1 allows 1 m long drift spaces for a peak current of 50 mA.

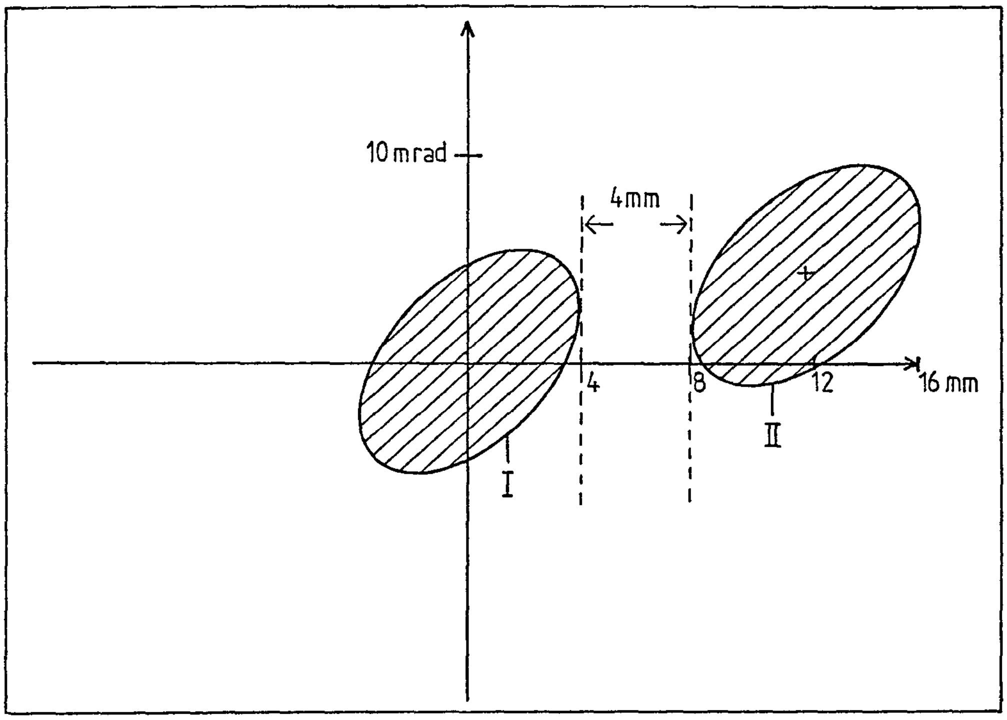

Fig. 2: Phase space diagram at the collector for the unchopped (I) and the chopped (II) beam.

The major disadvantage of this bunched beam transfer line is the emittance increase and the restrictions to the incoming emittances in all 3 planes. In the buncher cavities, both the transverse beam radius and the longitudinal phase width have to be limited. Transverse-longitudinal coupling, from the radial dependence of the transit time factor, and longitudinal aberration, due to the sinusoidal bunching field must be avoided. In order to install 1 m long drift spaces between the bunching cavities, the RFQ output normalised emittances have to be:

$$\varepsilon_t^{rms} \le 0.2\,\pi \text{ mm mrad}, \quad \varepsilon_L^{rms} \le 0.2\,\pi\,° \text{ MeV (400 MHz)}$$

For the transverse plane, this limits the geometrical emittance of the 100 keV ion source beam to a value difficult to fulfil for a 50 mA H^-pulse current source [4]:

$$\varepsilon_t^{ion\text{-}source} \le 55\,\pi \text{ mm mrad (geometrical, } 4 \cdot \text{rms-value)}$$

Due to the 50 mA peak current at 2.5 MeV, severe space charge forces are present. One quarter of the plasma wavelength, where most of the emittance increase occurs [9], is only about 0.3 m, and we cannot preserve the RFQ focusing period. Therefore the non-periodic transfer line suffers severe emittance increase caused by both the non-linear external bunching forces and the high internal space charge forces. Typically we find about 50% rms emittance increase in all 3 planes. It should be mentioned, that in the rms envelope equation the emittance term and the 50 mA space charge term are almost equal for the periodic part from the triplet (T) to triplet (T).

Most of the emittance increase may be reduced by shortening the line. For doing so, a more effective chopping structure with a voltage slope of about 200 V/nsec is needed. The now discrete buncher (B)-triplet(T)-buncher (B) combination should be replaced by a compact, non-accelerating RFQ-structure. A "pre-chopper" between ion source and RFQ should be installed to reduce the heat load at the collector.

The most promising alternative, however, is to use a coasting beam instead of a bunched beam. By doing so we can handle much larger transverse emittances, which put less demands on the development of high brilliance H^- sources. On the other hand, adiabatic trapping of a coasting beam in the DTL is a problem. Maybe it can be overcome by using first a bunch compression RFQ, where the coasting beam is compressed into a phase width of about ± 90° with almost no acceleration. This bunch can then be injected into the DTL by slowly increasing the synchronous phase from - 90° to - 25°. Studies are going on to evaluate this promising alternative in great detail.

2. Bunch Rotation and Energy Ramping at the Linac Output

The final linac energy of ≥ 0.8 GeV is achieved by changing the 400 MHz DTL structure at 100 MeV to a more efficient 800 MHz coupled cavity structure. Due to adiabatic phase damping, the outcoming linac bunches are narrow, with large values of energy spread. Typical numbers at 1 GeV are a phase width of ± 10° (800 MHz) or a bunch length of ± 75 psec and an energy spread of ± 2 MeV, corresponding to a momentum spread of ± $1.2 \cdot 10^{-3}$. As the bucket momentum height of the compressor ring is only about ± $5 \cdot 10^{-3}$, and as longitudinal painting [10] is essential for keeping the bunching factor small, the outcoming linac bunches have to be rotated in phase space and slow energy ramping used over the linac pulse. Both tasks may be fulfilled using a cavity which simultaneously rotates the bunch and slowly ramps the energy by varying amplitude and phase. The required cavity position and rotation voltage are strongly influenced by longitudinal space charge effects. Longitudinal aberration effects, caused by the sinusoidal voltage are discussed. The correct setting of the rotation voltage may be controlled on line by broadband pickups. In front of the cavity an achromatic bending system should be installed which allows the scraping of longitudinal halo particles.

a) Change of the Longitudinal Parameters Due to Space Charge Forces

As an example, Fig. 3 shows the increase of the phase width (in°) or the bunch length (in cm) in a longitudinal drift space for a 1.2 GeV beam, coming out of a 1200 MHz coupled cavity linac. The initial total phase width is assumed to be ± 6° (1200 MHz), the initial total energy spread to be ± 2.5 MeV. The solid line in Fig. 3 is the zero current case, whereas the broken line is calculated for 50 mA peak current in the 400 MHz DTL structure or 150 mA in 1200 MHz coupled cavity linac. The transverse beam radius is kept constant along the line. The space charge calculations are done with a numerical code, assuming linear space charge forces of a uniformly filled 3-dimensional ellipsoid. The variation of the phase width is taken into account. The code treats flat bunches with a large ratio of the longitudinal bunch length compared to the transverse beam radius. Due to the linear space charge forces, there is no emittance increase. Longitudinal space charge forces act as a linear defocusing lens with varying field strength along the line. They keep the longitudinal emittance constant, but they influence the phase width and the energy spread. The position of the bunch rotation cavity has to be changed, especially if the cavity operates at the 400 MHz DTL frequency. This would decrease the energy spread by a factor 8.

For most spallation source injectors, the energy spread has to be decreased only by a factor 2, allowing use of the same coupled cavity structure as before but now phased to - 90°. Fig. 4 and 5 show the use of such a 1200 MHz structure with somewhat changed input parameter ($\Delta\varphi$ = ± 8° (1200 MHz), ΔW = ± 2 MeV), calculated for the 150 mA peak current at 1200 MHz. The bunch rotation cavity is placed after 65 m and with a voltage of ~ 6 MV; the phase width afterwards is constant to about ± 40°. For a zero current beam, not shown, a phase width of ± 40° occurs after 107 m.

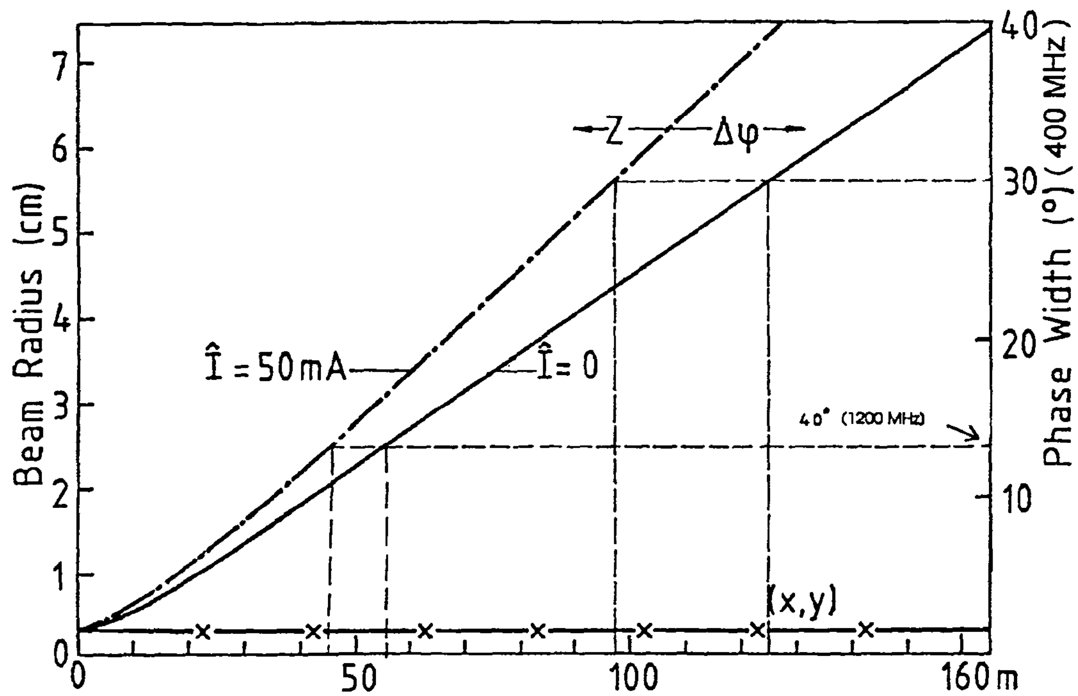

Fig. 3: Increase of the longitudinal phase width (√5·rms) for a 1.2 GeV beam with I = 0 and 50 mA

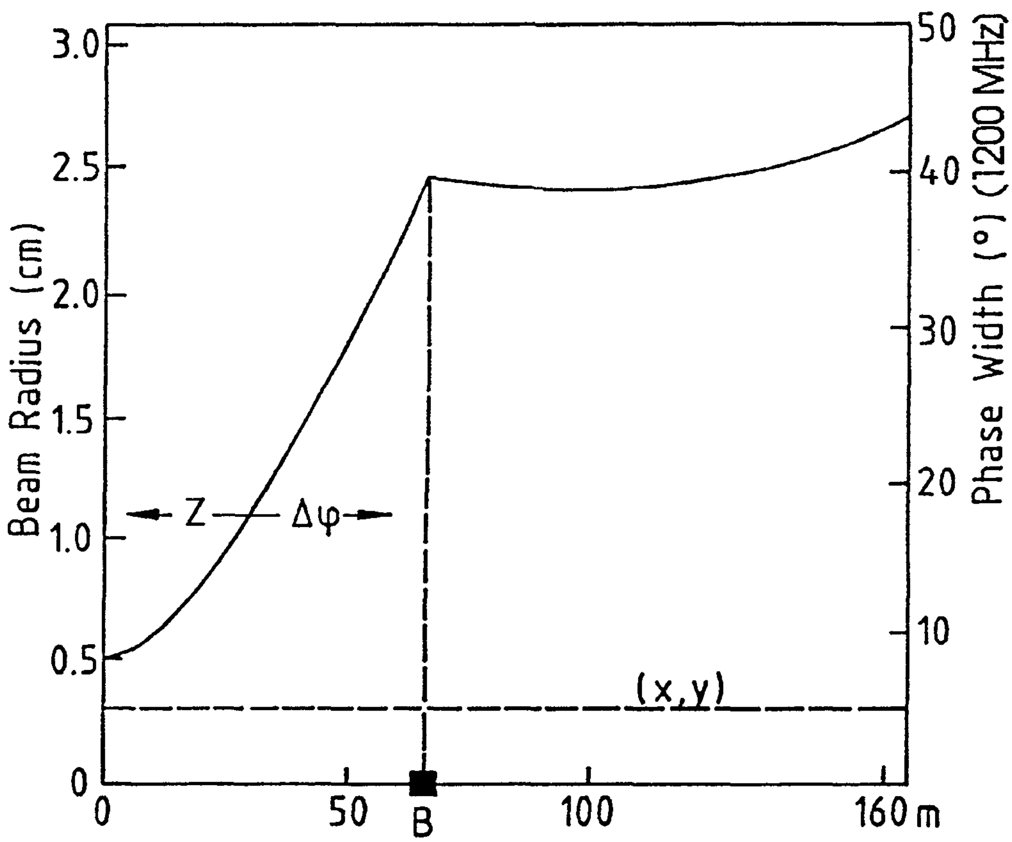

B: 1200 MHZ buncher L = 1.5m V ~ 6 MV

Fig. 4: Phase width (√5·rms) for 1.2 GeV and I = 150 mA using a 1200 MHz cavity

There is an accompanying increase of the energy spread, as shown in Fig. 5. Before the bunch rotation cavity, the energy spread is increased by a factor ~ 2; afterwards it is roughly constant, and at the end of the transfer line, the energy spread is reduced by more than a factor 2. The increase of the energy spread in front of the cavity doubles the required rotation voltage. If the space charge effects are ignored, the bunch rotation cavity is positioned incorrectly, with the cavity field non-linear. In addition, the foreseen voltage is too low, resulting in incomplete rotation, with longitudinal aberration effects as discussed later.

b) Analytical Formulae for the Description of the Longitudinal Space Charge Effects

As shown in Fig. 3 - 5, the phase width increases linearly at large distance, whereas the energy spread goes into saturation. This is expected because the space charge forces are getting weaker; the asymptotic behaviour may be described quite well by simple analytical formulae. For a longitudinal waist at the start, and for a final phase width $\Delta\varphi_f$ afterwards, the change of energy spread and the needed drift length L_D are given approximately by:

$$\left(\frac{\Delta W_f}{\Delta W_i}\right)^2 = 1+\left(\frac{\mu-1}{1+\alpha(I)\cdot\mu}\right)\left(1+\frac{1}{\alpha(I)\cdot\mu}\right) \tag{2}$$

$$L_D = \sqrt{\frac{\mu\cdot\beta_i}{f(I)}}\cdot \mathrm{sh}^{-1}\left(\sqrt{\frac{\mu-1}{1+\alpha(I)\cdot\mu}}\right) \tag{3}$$

with:

$$\mu = \left(\frac{\Delta\varphi_f}{\Delta\varphi_i}\right)^2 \qquad \frac{1}{\alpha(I)} = \beta_i\cdot f(I)$$

$$\beta_i = \frac{(\Delta\phi_i)^2\cdot\lambda\cdot(\beta\gamma)^3\cdot m_o c^2}{\left(E_z/\pi\right)\cdot 360^o} \qquad f(I) = \frac{120\cdot I\cdot 360^o\cdot\Omega\cdot q}{\beta\cdot\bar{a}\cdot\left(E_z/\pi\right)}$$

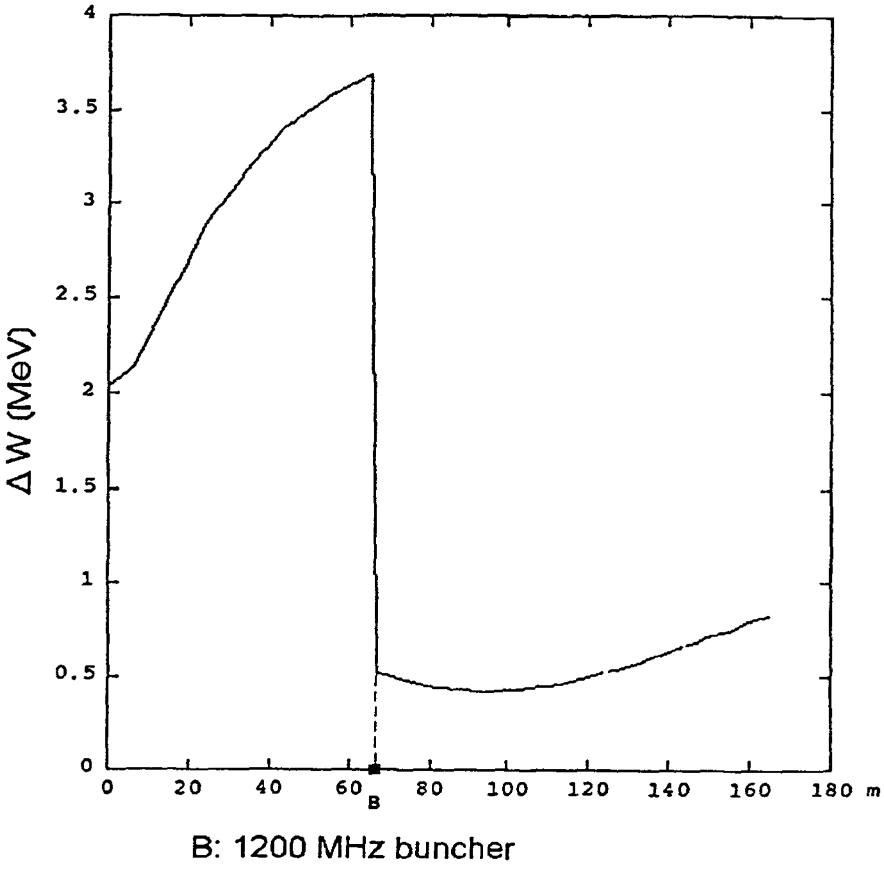

B: 1200 MHz buncher

Fig. 5: Energy Spread ($\sqrt{5}$·rms) for 1.2 GeV and I = 150 mA using a 1200 MHz cavity

$(\Delta\varphi_i, \Delta\varphi_f)$:	(initial, final) phase width (in°)
$(\Delta W_i, \Delta W_f)$:	(initial, final) energy spread (in MeV)
β_i:	initial longitudinal β-function (in m)
E_z:	longitudinal phase space area (in °MEV) = $\pi \cdot \Delta\varphi_i \cdot \Delta W_i$
λ:	wavelength of the rotating cavity
I:	peak current
$\bar{a} = \sqrt{a_x \cdot a_y}$:	average transverse beam radius
(β, γ)·	relativistic factors
$(m_o c^2, q)$:	(rest mass, charge) of the particle
$(\Delta\varphi, \Delta W, \bar{a})$ =	$\sqrt{5}(\Delta\varphi, \Delta W, \bar{a})_{rms}$
E_z=	$5\ E_z^{rms}$

Eq (2,3) are correct for $\Delta\varphi_f > 3 \cdot \Delta\varphi_{i.}$·

They are derived by averaging the longitudinal space charge force over the drift distance [1] assuming a homogenous filled 3 dimensional ellipsoid. The final phase width $\Delta\varphi_f$ is treated as input parameter, giving the needed drift length L_D as an output parameter.

For very large values of $\Delta\varphi_f$, where the following holds, Eq (2,3) can be written as

$$\alpha(I)\cdot\left(\frac{\Delta\varphi_f}{\Delta\varphi_i}\right)^2 >> 1$$

$$\left(\frac{\Delta W_f}{\Delta W_i}\right)^2 = 1+\beta_i\cdot f(I) \tag{4}$$

$$L_D = \left(\frac{\Delta\varphi_f}{\Delta\varphi_i}\right)\cdot\sqrt{\frac{\beta_i}{f(I)}}\,\mathrm{sh}^{-1}\left(\sqrt{\beta_i\cdot f(I)}\right) \tag{5}$$

This is the asymptotic case, where the energy spread becomes constant, depending only on the initial conditions. The phase width $\Delta\varphi_f$ increases linearly with the drift distance. The zero current case can be obtained from Eq (4,5) by setting the peak current to zero. These simple analytical formulae describe the longitudinal space charge effects quite well. For example with the same input data as for the numerical calculations of Fig. 4 and 5, we get:

$$\text{for } \hat{I} = 150\text{mA}, \Delta\varphi_i = \pm 8^\circ, \Delta W_i = \pm 2\text{MeV}, T = 1.2\text{GeV}, \bar{\alpha} = 3\text{mm}$$

$$\beta_i = 21.8\text{m} \qquad f(I) = 0.0144\,{}^1\!/_{\text{m}} \qquad \alpha(I) = 0.315$$

which means that we reach the final phase width $\Delta\varphi_f$ = ± 40° after L_D = 78 m with an energy spread of ΔW_f = ±4.1 MeV. The energy spread has almost reached its asymptotic value of ± 4.16 MeV. The numerical calculations, see Figs. 4,5, gives a driftlength of 65 m and a energy spread of ± 3.7 MeV. Also here the energy spread is approaching the constant asymptotic regime.

For a zero current beam, the drift length L_D is given by

$$L_D = \sqrt{\beta_i(\beta_f - \beta_i)} \tag{6}$$

where $\beta_f \sim \Delta\varphi_f^2$ is the final longitudinal β-function. A phase width of ± 40° is reached after 107 m. After the bunch rotation cavity, where the phase width stays almost constant, Eq (4) cannot be used. Here the change of the energy spread, see Fig. 5, can be described by a similar equation, using the longitudinal form factor of a "flat" bunch.

The simple analytical formulae allow the energy spread and the position of the bunch rotation cavity to be calculated for a given beam current and phase width at the cavity position. Beside the initial longitudinal β-function, only one current dependent factor must be calculated.

All numerical and analytical space charge calculations presented are made for linear forces without emittance increase. Longitudinal emittance increase has to be calculated by multiparticle codes, where the distribution at the linac output has to be taken as initial conditions. Thus, the beam has to be simulated throughout the linac, including the low energy matching sections. For locating the bunch rotation cavity and choosing the correct voltage, not much difference is expected from the presented linear space charge analysis.

c. Longitudinal Aberration Effects and Energy Ramping

The non-linear part of the voltage must be taken into account, especially for large voltages and bunch lengths. The sinusoidal voltage leads to longitudinal aberration effects and a dilution of the phase space area. For a linear voltage and an elliptical phase space boundary at the cavity entrance, there is an upright ellipse afterwards, where the outermost particles have no energy spread. The maximum energy spread is determined by the particles in the bunch centre. For a sinusoidal voltage, there is no longer an elliptical boundary afterwards. Keeping the same voltage as for the linear case, the outermost particles are no longer on axis. For the values of Fig. 5: U = 6 MV, $\Delta\varphi$ ± 40°, this gives for the outermost particle an energy spread of ± 300 keV compared to ± 550 keV for the bunch centre, which is acceptable.

The required slow energy ramping of the linac pulse, essential for the longitudinal painting [10], may be done by using either the bunch rotation cavity or the last part of the coupled cavity linac. In both cases, the synchronous phase (and the amplitude) are slowly changed during the linac pulse. If the bunch rotation cavity is used for energy ramping, aberration effects have to be taken seriously. Using the data of Figs. 4 and 5 as an example; by ramping the phase from - 65° to - 90° to - 115° and the voltage from 6.7 to 5.3 to 6.7 MV, the energy can be varied from + 3 to 0 to - 3 MeV. The incoming bunches may still be rotated ($\Delta\varphi = \pm 40°$, $\Delta W = \pm 3.7$ MeV), but due to the strong aberration effects, the phase space boundary is no longer elliptical. For the energy ramped bunches, an almost rectangular phase space boundary is obtained, whereas the unramped bunches keep their elliptical boundary. The energy spread obtained, however, is still below ± 1 MeV for all bunches.

These results may be compared with the alternative of using the coupled cavity structure instead. Here aberration effects are almost non existent due to the small phase width around ± 10°. The synchronous phase may be changed adiabatically over many cells. Due to the use of large peakpower klystron units, the cells are grouped together in accelerating tanks having a common phase. Longitudinal mismatch effects cannot then be avoided. In a coupled cavity tank, where there is an energy gain of 18 MeV (total voltage 20 MV, synchronous phase - 25°), the energy may change only by an additional ± 1 MeV. Even then, the ramped bunches are mismatched at the linac exit and, due to the space charge forces, this longitudinal mismatch is increased up to the position of the bunch rotation cavity. After the rotation, all bunches have an elliptical boundary, but, due to mismatch, different energy spreads. This may be overcome by varying the amplitude of the bunch rotation cavity in an appropriate way, though for large values of the mismatched phase width, aberration effects have also to be considered. Detailed numerical calculations, including space charge and aberration effects, are proceeding to compare both possibilities for energy ramping to find the optimized voltage and phase programmes.

d) Online Measurements of the Longitudinal Beam Parameters and Longitudinal Halo Scraping

Due to the effects of space charge forces, it is important to measure the beam parameters online, especially to obtain the correct voltage setting. The online measurement may be done using broadband high frequency pickups (up to 6 GHz) and reconstruction methods in the frequency domain [12]. From the low frequency components of one pickup, the rms phase width is obtained, and by using, in addition, the high frequency content, the bunch distribution also. The reconstruction method has recently been confirmed with beam at the ISIS-facility [13]. With two identical pickups, the rms energy spread is obtained, and by placing identical broadband pickups before and after the bunch rotation cavity, the longitudinal beam parameters are measured on line for control of the rotation voltage.

Along the spallation neutron source linac, there is normally more longitudinal than transverse emittance increase. The longitudinal acceptance is too small at low energies and high intensities [14]. The frequency jump of the accelerating structures, in order to make the linac more cost effective, causes aberrations. To keep injection loss small in the subsequent rings, it is very desirable to scrape the longitudinal H^- halo particles, by stripping. This may be achieved by including an achromatic bending system in the high energy transfer line as in the PSR [15]. Care has to be taken in the design, as the bending field strength is limited to avoid unwanted Lorentz stripping of the H^-ions, and there is also length limitations. Due to the space charge forces, the energy spread is large and approximately constant only after the rotation cavity.

As an example, at 1.2 GeV, we can design a short 4 cell achromatic bending system, corrected in first order and only 36 m long [16]. This device has in the middle a dispersion value of about 1.6 m compared to the horizontal β-function value of 2.6 m, sufficient for doing the longitudinal halo scraping. The bending field is 0.3 T, which limits the stripping loss below 10^{-6}/m for the complete achromatic bending system. Over the total length of 36 m, the energy spread increases by 20%, see Fig. 5. Due to transverse-longitudinal coupling in the dispersive elements, only the 4-dimensional phase space area is conserved, but not the 2-dimensional projections on the transverse or the longitudinal plane. By choosing proper settings of the elements, we can preserve either the transverse or the longitudinal emittance [17]. Work is proceeding to find, under the space charge forces, the optimal parameters by looking at the transverse and the longitudinal plane simultaneously.

Summary

Major arguments are given on how to include a fast beam chopper at low energies and a bunch rotation cavity at high energies when both these linac areas are dominated by space charge forces. Careful design of these sections is important for loss-free injection and extraction in the subsequent rings for the next generation spallation neutron source.

Acknowledgement

Most of the work presented resulted from lively, exciting, fruitful discussions with colleagues from the former EHF study group, which was led by F. Bradamante, who is accordingly thanked.

References

[1] G. Rees, "Overview of Future Spallation Neutron Sources", to be published in: Proc. of the US Particle Accelerator Conferences, 1993.

[2] H. Lengeler, "The European Spallation Source Project ESS", invited talk at ICANS XII

S. Martin, C. W. Planner "Accelerator Design Parameters for a European Pulsed Spallation Neutron Source", Proc. EPAC Berlin 1992, p, 435

[3] J. M. Brennan, L. Ahrens, J. Alessi, J. Brodowski, J. Kats "A Fast Chopper for Programmed Population of the Longitudinal Phase Space of the AGS Booster", Proc. EPAC Rome 88, p. 1003

[4] D. Schneider "Summary Report: Ion Source", Proc. Spallation Source Workshop, Santa Fe 1993, Los Alamos Conference Report, LA-UR-93-1356, p.1

[5] T. Weis, J. Wiegand, R. Dölling, J. Pozimski, F. Fenger, H. Klein "Evaluation of Space Charge Neutralization in a High Perveance Injector System with Solenoids" Proc. EPAC Nice 1990, p. 809

[6] J. S. Lunsford, R. A. Hardekopf "Pulsed Beam Chopper for the PSR at LAMPF", Proc. 1983 Particle Accelerator Conference, IEEE NS-30,(1983) p.2830

[7] K. Bongardt, M. Pabst, R. Wagner "The 2,5 MeV Low Energy and the 1,2 GeV High Energy Transfer Lines", Proc. International Workshop on Hadron Facility Technology, Santa Fe 1987, Los Alamos Conference Report LA-11130-C, p. 184

[8] F. Bradamante "Meson Factories", Proc. EPAC Rome 1988, p.70

"Proposal for a European Hadron Facility", Edited by J. F. Crawford, EHF-87-18, May 18, 1987.

[9] T. P. Wangler, K. R. Crandall, R. S. Mills "Emittance Growth from Charge Density Changes in High-Current Beams", Proc. Heavy Ion Inertial Fusion 1986, AIP conference proc. 152, (1986), p. 166

[10] E. Gianfelice, H. Schönauer "Strategies for Longitudinal Painting in the EHF Booster at Injection", Proc. EPAC Rome 1988, p. 860.

[11] K. Bongardt "Design Formulae for a Space-Charge Dominated Transport Line", internal KFA Jülich note, Nov. 1988.

[12] K. Bongardt, A. K. Mitra, M. Sauer, H. Stockhorst "The Deflector-Pickup System: A Novel Approach to Measure Online the Energy Spread of DC Ions Beams", NIM A 287, (1990), p. 273.

K. Bongardt, K. Kennepohl "Determination of 100 psec Short Linac Bunches by Broadband Pickups and Reconstruction Technique", Proc. EPAC Rome 1988, p. 976.

[13] M. Clarke-Gayther, private communication

[14] M. Pabst, K. Bongardt, U. Funk "An Improved Definition of the Longitudinal Acceptance for High Intensity Bunched Beams", Proc. Workshop on High-current, High-Brightness and High-Duty-factor Ion Injectors, AIP Conference Proceedings 139, (1985), p. 193.

[15] G. P. Lawrence, R. A. Hardekopf, A. J. Jason, P. N. Clout, G. A. Sawyer "Los Alamos High-Current Proton Storage Ring: A Status Report", Proc. Particle Accelerator Conference 1985, IEEE NS-32, (1985), p. 2662

[16] J. Crawford "Achromat Between the EHF Linac and Booster", EHF-88-4, Feb. 1988

[17] A. J. Jason, E. M. Svaton, B. Blind, E. A. Heighway "Design of Achromatic Bending Systems in the presence of Space Charge", Proc. Particle Accelerator Conference 1987, p. 1767 .